

Practical Cellular Performance Bounds via Shotgun Cellular Systems

Timothy X Brown¹

Dept. of Electrical and Computer Engineering
University of Colorado, Boulder, CO 80309-0530
timxb@colorado.edu

Abstract

This paper considers two-dimensional interference-limited cellular radio systems. It introduces the shotgun cellular system that places base stations randomly and assigns channels randomly. Such systems are shown to provide lower bounds to cellular performance that are easy to compute, independent of shadow fading, and apply to a number of design scenarios. Traditional hexagonal systems provide an upper performance bound. The difference between upper and lower bounds is small under operating conditions typical in modern TDMA and CDMA cellular systems. Furthermore, in the strong shadow fading limit the bounds converge. To give insights into the design of practical systems, several variations are explored including mobile access methods, sectorizing, channel assignments, and placement with deviations. Together these results indicate cellular performance is very robust and little is lost in making rapid minimally-planned deployments.

1. This work was completed under NSF CAREER Award NCR-9624791 and NSF Grant NCR-9725778.

1. Introduction

Optimal planar cellular systems place *base stations* (BS) in uniform size hexagonal grids [10, 13, 14, 16, 18]. Current cellular and PCS systems, with their small cell sizes, depart significantly from the ideal hexagonal layout due to terrain variations, difficulties in site acquisition, and time-to-market constraints in the competitive PCS market. Space variations in *mobile station* (MS) density add varying cell-sizes. In low-power PCS systems, “referring to average coverage area shapes as circles, squares, or hexagons surrounding [BS] is a largely academic exercise” [8]. In quickly deployed ad hoc military or emergency communication systems, little or no planning is possible. Distributed campus wireless LANs may add communication elements in a distributed fashion with little coordination between departments. Study of cellular system performance has been limited to analysis and simulation studies of idealized system types or specific instances (e.g. [2, 6, 7, 10, 11, 13, 14, 16, 18]). While the best performance we can achieve is given by the hexagonal system, what lower bounds the performance? Under typical conditions, how much performance can we lose or gain between different cellular designs?

To proceed we need to define the design problem and performance measures. A cellular design includes factors such as tower construction, radio and antenna types, available bandwidth, and traffic loads. Within such factors, the design centers on the problem of placing BS and assigning channels to BS.

Given a set of BS that provide radio coverage over the plane, this paper examines channel assignments that are fixed over a design period². A number of factors affect channel assignment. Different BS may require more or less channels. Different services may require more or less channel resources. But, the essential elements of a fixed channel assignment can be modeled as follows. Divide the available channels into a fixed number of *channel reuse groups* (CG) and assign each BS one CG. If divided into more CG, co-channel groups can be separated more, reducing interference, and increasing signal quality. Signal quality can be made arbitrarily high with increasing number of CG. Unfortunately, with more CG the number of channels per CG is less, reducing the number of channels per BS, and reducing spectrum efficiency (capacity). Therefore, design performance is defined by the signal quality distribution as a function of number of CG.

BS are not placed arbitrarily. They are distributed across the plane to meet traffic and cover-

2. For dynamic channel assignment within the shotgun framework see [4].

age requirements. In the *noise limited* case, performance is limited by the ability to have sufficiently strong signals over the coverage area. The goal is to achieve coverage over the plane with the least number of BS within the limits of BS range. In other words, the goal is to have the largest average coverage area per BS for a given maximum range. In the *interference limited* case, performance is limited by the interference from the many co-channel radios. The goal is to capture the offered traffic load with the least number of BS within the limits of only one CG per BS. The number of BS are minimized by having the most channels per CG. In other words, the goal is to have the fewest CG to meet a given required signal quality. Much of the design work in practical systems is used to ensure adequate coverage. Based on the examples at the beginning, this paper focusses on the interference-limited case where we assume that BS density is high enough that coverage is not the primary issue and instead interference is the issue.

Even in a generally flat plane, local terrain and clutter cause dramatic spatial variations in the received power [7,21]. In interference limited systems, these variations can lead to MS communicating not with the nearest BS (which may be blocked by a large building) but with a further BS (which might have a less obstructed path) [2]. Such so-called *shadow fading* is a significant factor in any cellular design. Combining these elements, BS placement and CG assignment algorithms are ranked by the signal quality distribution as a function of the number of CG under shadow fading in an interference limited environment.

This paper develops and analyzes both upper and lower performance bounds to practical interference-limited cellular systems. The upper bound is the performance of BS placed on an ideal flat plane in a uniform-size regular hexagonal grid. The lower bound places BS randomly and assigns CG randomly (as in the random shot pattern of a shotgun). We show that the lower bound performance is independent of shadow fading and all systems converge to the lower bound in the limit of large shadow fading variation. The bounds apply to cellular variations including sectoring and mobile access strategy. Channel assignment's effect and placement's effect on the bounds is tested via non-random channel assignment in the shotgun system and placement with deviations in the hexagonal case.

The paper elaborates the system model in Section 2, derives shotgun system performance in Section 3, analyzes shadowing in Section 4, studies upper and lower performance bounds in Section 5, applies several design variations in Section 6, and concludes with Section 7. To focus on the main results, the mathematical analysis is found in the Appendices.

2. Model

This section describes the details of the model used for the paper's results. The model elements include BS layout, CG assignment, radio environment, traffic, performance measures, and mobile access strategy. We discuss each element in turn. Conceptually, the model is a low-power high-density grid of BS. See papers by Cox [7, 8] and references therein for further background on such a model. The overriding goal is to develop a model that strips away all but the most relevant features of a cellular system. The rest of this section justifies each element to the model and the model is summarized in Section 2.7.

2.1 BS Layout

The shotgun system distributes BS across the plane as a 2-D Poisson point process, where the average density of stations is λ and the probability of a BS in a small area dA is λdA . See Appendix A for properties of this process. This results in local sparse and dense concentrations of BS as might follow in a practical system due to terrain and traffic variations. The hexagonal layout places cells according to a regular hexagonal grid. Deviations from an ideal hexagonal grid are discussed in Section 6.4. The cellular systems extend in all directions over the plane.

2.2 CG Assignment

This paper is restricted to fixed channel assignments that assign one of N orthogonal CG to each BS. In an FDMA-based cellular system, each CG is a set of frequency channels. In a TDMA-based cellular system each CG is a set of frequency and time-slot pairs. In a CDMA-based cellular system each CG is a set of frequency channels which in turn carry multiple users via spread spectrum techniques.

The shotgun system randomly assigns CG according to a uniform distribution. The hexagonal system achieves good channel assignment only for certain N and only then with particular channel assignment patterns [13, 16, 18]. The first 10 valid N are 1, 3, 4, 7, 9, 12, 13, 16, 19, and 21. Non-random assignment in the shotgun system and random assignments in the hexagonal system are discussed in Section 6.3.

2.3 Radio Environment

All BS have identical transmit power, antenna gains, etc., and the path loss is an inverse power law with path loss exponent ϵ . All antennas are omnidirectional with no variation in the vertical radiation pattern. Sectorized antennas are discussed in Section 6.2. The CG are perfectly orthogonal so that adjacent channel interference is ignored and only co-channel interference is consid-

ered. Since this paper focuses on dense interference-limited systems, background and thermal noise are assumed zero. Rayleigh fading (aka small-scale fading [21]) is treated by micro-diversity techniques in the radio channel and considered outside the scope of this paper (so-called local mean statistics [2]).

Shadow fading (aka large-scale fading) is modeled as independent log-normally distributed multiplicative noise, Ψ , on the signal strength received from each BS. It is well modeled by a log-normal density [7,21]:

$$p(\Psi) = \frac{1}{\Psi \sqrt{2\pi\sigma}} e^{-\frac{1}{2}\left(\frac{\ln\Psi}{\sigma}\right)^2}, \quad (1)$$

so that the signal has mean 1 and one standard deviation includes from $1/\sigma$ to σ . The shadowing process captures variations due to terrain and clutter between the BS and MS. It does not depend significantly on the channel frequency. The shadow fading between each BS and MS pair is uncorrelated.

With this radio model, the received power is simply

$$P = \frac{K\Psi}{R^\epsilon}, \quad (2)$$

where K is a constant that embodies factors such as transmitter power and antenna gains that are the same on every link, Ψ is the random shadow fading factor, and R is the transmitter to receiver separation.

2.4 Traffic

To fully develop this problem's traffic characteristics we would need to define the Erlangs of offered traffic per BS or the distribution of offered traffic over the plane, and the number of traffic channels per CG. In order to make the basic results as clear as possible we use the following simple model.

Consider an offered load of 95 Erlangs per BS and 100 channels per CG. According to the Erlang B formula, some channel is available in each BS 95% of the time while any given channel is in use 90% of the time [16 p. 422, 18 p. 49]. Modern digital cellular systems can have well over 100 channels per cell. Increasing the offered load and the number of channels appropriately, we arrive at the following *many-channel limit*. Every BS has an available channel with probability close to one and any given channel is occupied with probability close to one. Thus, every BS has some channel available and every possible interfering co-channel cell is occupied. This limit

allows us to use the number of CG to compare capacity of cellular systems without the relatively minor variations imposed by specific values for number of channels and offered loads. With this traffic model, we measure the performance of a single MS, at a random instant in time, uniformly distributed over the plane.

2.5 Performance Measures

Performance measures in cellular focus on capacity and signal quality. Signal quality is indicated by measures such as signal to noise plus interference, signal to distortion [2], bit or frame error rates for digital traffic, or speech quality measures for voice traffic. [18, p. 389]. Signal to distortion includes delay spreads that depend on specifics of the environment, are relatively insensitive to BS layout, and if problematic are ultimately treated with equalization. Most measures such as error rates and subjective quality ultimately can be translated to measures of signal to noise plus interference. In an interference limited cellular system, noise is inconsequential compared to the interference from co-channel BS assigned the same CG. Thus, we measure signal quality by the received signal power compared to the interference which we denote the carrier to interference ratio (C/I). The C/I for a given BS to MS connection is:

$$C/I = \Psi_S R_S^{-\epsilon} / \sum_i \Psi_i R_i^{-\epsilon} , \quad (3)$$

where R_S is the distance to the signal BS, $\{R_i\}$ is the set of distances to co-channel interfering BS, and the Ψ are the corresponding fading components. The C/I in (3) depends on scale invariant distance ratios. As a result, the C/I distribution is independent of the BS density, λ .

Assuming the number of orthogonal channels is fixed, a measure that captures cellular system differences is the number of CG (i.e. N) required to meet a particular C/I ratio for a given fraction of users. Larger N yields fewer channels per CG and thus fewer channels per BS and less capacity. Smaller N yields the opposite. Conversely, another measure is the C/I that a given fraction of users exceed for a given N . Both of these measures are coupled directly to the C/I distribution as a function of N . This paper uses the C/I distribution at the 95th percentile. This is a balance between older systems that designed for the 90th percentile [14] and newer systems that compete with wireline and design at the 98th or 99th percentile [2].

The C/I can be measured on the BS to MS downlink or the MS to BS uplink. Given a set of BS, the location of the MS determines the downlink C/I in (3). The uplink C/I , on the other hand, requires the additional knowledge of the location of every active MS and BS pair. An uplink study

is only possible through detailed traffic-based simulation, while the downlink may yield to analysis or at least much simpler and more transparent simulations. A detailed simulation in [4] looked at both the uplink and downlink with this model. It found that the performance differed slightly between the uplink and downlink, but qualitatively they are similar. For these reasons we focus only on the downlink.

2.6 Mobile Access Strategy

At call set up—or at any point afterwards when the MS might reassess its channel assignment—the MS chooses the CG that provides the highest C/I. Given the traffic and performance measures, this maximizes the C/I distribution for the MS. Another protocol is considered in Section 6.1. The details of how the MS makes the assessment is not relevant. But, it may be helpful to think of a control channel in each CG. The MS monitors the N control channels in turn and estimates metrics such as the frame error rate that indicates C/I.

2.7 Model Summary:

This paper analyzes the downlink C/I distribution as a function of the number of CG, N , for C/I defined by (3) and model instances characterized by the following variables and options:

- BS layout/CG Assignment: Shotgun or regular hexagon.
- Radio Environment: Path loss exponent, ϵ , shadow fading standard deviation, σ in dB.

The shotgun and hexagonal scenarios are denoted as SG and HEX respectively. Simulations based on these models use the methodology described in Appendix B. Variations on the basic model are discussed in Section 6. Clearly, many cellular details have been stripped away. But, what remains are the characteristic elements that fundamentally distinguish the cellular environment.

3. Shotgun Performance Under No Shadow Fading

This section analyzes the shotgun cellular C/I distribution and shows that it is easy to compute. The analysis starts with only a signal BS and the first closest interferer and then extends the analysis to BS covering the entire plane. The shadow fading standard deviation is zero. Non-zero shadow fading standard deviation is treated in the next section.

First consider identical omni-directional BS all using the same CG ($N = 1$). The C/I is maximized by choosing the nearest BS as the signal with the next nearest as the interference. As a worst case, the two nearest BS are at the same distance so that the signal to interference is greater than or equal to 1. For a random MS on the plane, let R_1 and R_2 be the distance to the nearest and

next nearest BS. Using (3) and equation (15) in Appendix A, for $y \geq 1$:

$$\text{Prob}\left\{\frac{C}{I} > y|\epsilon\right\} = \text{Prob}\left\{\left(\frac{R_2}{R_1}\right)^\epsilon > y\right\} = \frac{1}{y^{2/\epsilon}}. \quad (4)$$

Performance with multiple CG depends on how the CG are assigned. The shotgun system assigns one of N CG to each BS from an i.i.d. distribution with p_i the probability of choosing CG i . Under the Poisson BS placement process, the BS assigned CG i can be modeled via a Poisson point process with BS density $p_i\lambda$; *independent* of any of the other CG. This implies that each CG produces an independent C/I sample each distributed as (4). The MS chooses the CG with the best C/I. It follows from (4) that with N CG,

$$\text{Prob}\left\{\frac{C}{I} > y|\epsilon, N\right\} = 1 - \left(1 - \frac{1}{y^{2/\epsilon}}\right)^N. \quad (5)$$

As in standard cellular systems, with large enough N any desired signal level can be achieved with high probability.

These results for the signal and first interferer extend naturally to a complete shotgun system. For a single CG, Appendix C, computes the C/I distribution for all BS as:

$$\text{Prob}\left\{\frac{C}{I} > y|\epsilon\right\} = \frac{K_\epsilon}{y^{2/\epsilon}}, \quad (6)$$

where $y > 1$ and K_ϵ is a constant less than one that depends on the path loss exponent. Figure 4 in Appendix C graphs K_ϵ . Surprisingly, the distribution retains the same form as (4). It follows that the C/I distribution with N CG when MS choose the BS with the best C/I is:

$$\text{Prob}_{\text{Best}}\left\{\frac{C}{I} > y|\epsilon, N\right\} = 1 - \left(1 - \frac{K_\epsilon}{y^{2/\epsilon}}\right)^N. \quad (7)$$

From (7) we conclude that the C/I distribution is easily computed for any path loss exponent or number of channel groups.

4. Shadow Fading

Shadow fading is the large-scale signal variation as a function of BS and MS location (e.g. whether indoors or outdoors, and what clutter and obstructions are in the signal path). It does not include the mean signal level dependence on distance. This section shows that while these variations have a detrimental impact on hexagonal system performance, the shotgun cellular performance is independent of shadow fading.

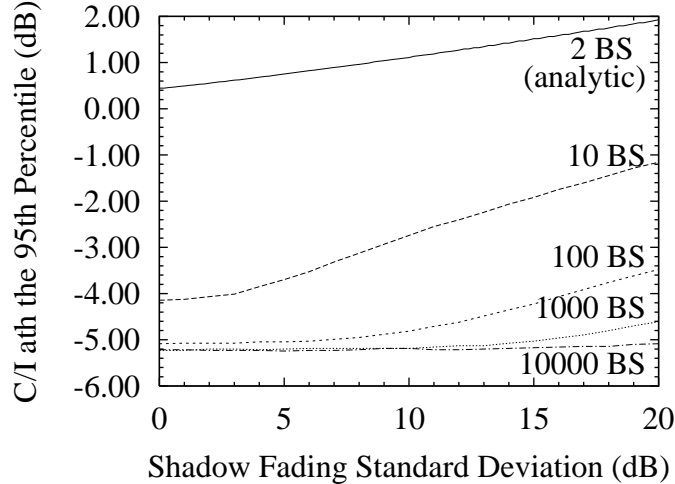


Figure 1: The C/I at the 95th percentile in the shotgun cellular system, for $N = 1$ CG, as a function of number of BS and shadow fading standard deviation, σ .

Statistically, shadow fading is well modeled by a log-normally distributed multiplicative variable on the received signal strength with density (1) [7, 19, 20]. In dB it is a zero mean, σ_{dB} standard deviation Gaussian random variable. Note that in (1), $\sigma = (\sigma_{\text{dB}}/10)\ln 10$. In hexagonal systems, shadow fading reduces the C/I that most users will receive and increases the number of CG needed for a C/I that a given fraction of users will receive [11].

For the shotgun cellular system we first analyze only the closest BS and the nearest interferer. Appendix D computes the C/I distribution if shadowing is introduced to (4). The resulting distribution is given in (23). It is possible, due to shadowing, that the further BS is stronger than the nearer BS so that the MS communicates with the further BS. In the limit of or $\sigma \rightarrow \infty$, the probability C/I is greater than any fixed level is 1. In other words, with a small number of BS, shadow fading has the potential to improve performance.

No analytic solution was found for the full shotgun system with shadow fading. We suspect that one exists based on the following empirical results. Figure 1 plots the C/I at the 95th percentile as a function of number of BS and shadow fading standard deviation. Similar graphs can be produced using different percentiles, number of channel groups, path loss exponents, etc. Such graphs show that in the limit of BS covering the plane (number of BS $\rightarrow \infty$), the C/I distribution is a constant. Further, this limit is approached from above. In other words, equation (7) characterizes the performance of the shotgun cellular system independent of shadow fading for infinite systems and bounds it from below for finite systems.

For cases where closed form solutions such as (7) are not available, we note that to accurately simulate the limit performance under shadow fading would require at least 1000 BS. Without shadow fading, 100 BS provides a performance estimate within a few tenths of a dB. Based on Figure 1, estimates without shadowing also estimate performance with shadowing. Therefore, even when simulations are necessary to estimate the shotgun performance, faster simulations with no shadowing and only a relatively few BS can estimate performance for any level of shadowing.

5. Upper and Lower Bounds on Practical System Performance

This section shows hexagonal and shotgun systems bound practical system performance, the difference in the bounds is small under typical situations, and in the limit of strong shadow fading all systems converge in performance to the shotgun system.

The hexagonal geometry is generally considered the ideal geometry for planar cellular systems [13, 16, 18]. Among BS placements, it yields the most compact geometry (i.e. ratio of cell radius to cell area). For certain number of CG, optimal CG assignments are known and such systems are generally regarded as having the best performance. Practical systems can not achieve this ideal due to terrain, political, and economic constraints. These constraints cause cell system designers to deviate from hexagonal, to substitute lower performance alternatives such as square grids, or to abandon any regular grid and build cells as coverage and capacity needs dictate. Thus, the performance of a hexagonal system on a flat plane upper bounds the performance we would expect in practice.

Practical system designers typically invest significant resources to plan and optimize their system within the above constraints. For these resources to have value, the performance of such systems exceeds shotgun systems that randomly distributes BS and CG. Worse performance is possible (for instance by throwing away some of the CG to maximize interference). But, this is a lower bound in the sense that any rational channel or spatial planning would only improve the shotgun system's performance. In the shotgun system, the underlying terrain is assumed planar. More realistic terrain is modeled by the log-normal shadow fading. But as seen in the previous section, shadow fading has no affect on the shotgun system performance and we can use (7) as a lower performance bound. Thus, we conclude that we can use ideal hexagonal and shotgun performance as bounds on practical system performance.

As seen in the previous section, hexagonal performance deteriorates with increasing shadow fading variance while shotgun performance is a constant. We might expect that the two perfor-

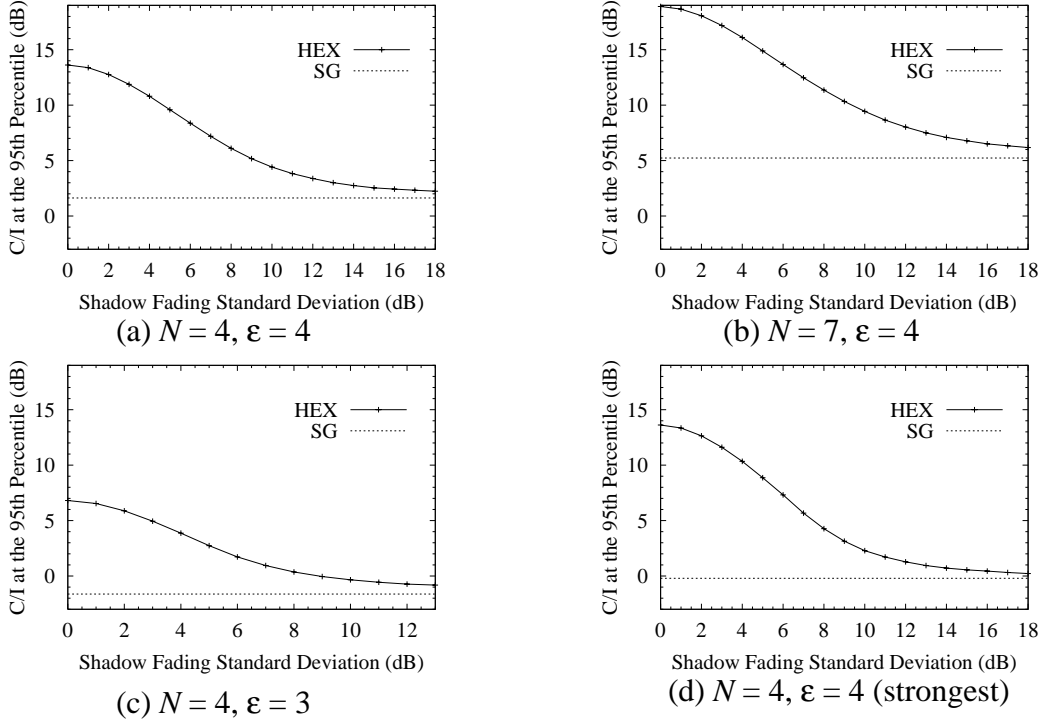


Figure 2: C/I at the 95th percentile as a function of shadow fading standard deviation for hexagonal (HEX), and shotgun (SG) systems. In all cases, the hexagonal performance converges to the shotgun performance in the limit of strong shadowing.

mances converge in the limit of high shadow fading standard deviation. This effect is indeed shown in Figure 2a–c for different number of CG and path loss exponents. The hexagonal performance is simulated while the shotgun performance bound is from (7)³. In the plots, the hexagonal performance degrades quickly over the first 10dB. Shadow-fading can range from 5–16 dB with $\sigma = 10$ dB being typical [7, 19, 20]. At 10dB the performance gap between the upper and lower bounds is a few dB and narrows with increasing σ . This behavior is observed across a number of scenarios. For instance, in Figure 2d we use the alternate channel access method described in Section 6.1 to produce a similar plot. Since practical systems fall somewhere within these narrow bounds, we conclude that practical system performance is characterized within a few dB by the shotgun cellular performance.

6. Cellular Design Variations

This section presents four different design variations; MS access method, sectoring, channel

3. In Figure 2c, the resulting C/I is less than 0dB where (7) is not valid, and the shotgun results are from a single simulation at $\sigma = 0$. Also, only $\sigma < 13$ dB is shown since with the smaller ϵ , signals attenuate less with distance and greater than 10^5 BS are required for the convergence at large σ shown in Figure 1.

assignment algorithms, and hexagonal placement with deviations. The section finishes with results from applying the variations. These show the effect on performance, and demonstrate the utility and limitations of the shotgun system model for making predictions.

6.1 Access Method

The paper has so far focussed on the MS choosing the BS that provides the best C/I. This is not necessarily the BS with the strongest signal power. Obviously, choosing the best C/I maximizes the MS C/I. But, not all air interface standards are capable of this strategy. For instance, early analog standards choose the BS with the strongest signal [14]. For clarity we call choosing the strongest BS the *strongest* strategy while the baseline strategy of choosing the BS with the best C/I we call the *best* strategy. This section looks at the performance loss incurred by the strongest versus best strategy and shows the strongest can be much worse, although it exhibits an independence to shadow fading like the best strategy.

Without shadow fading the strongest BS corresponds to the closest BS. In hexagonal systems without fading the closest BS is always the best BS so that without shadowing the best and strongest strategies are the same. In the shotgun system the access strategies are not the same. Considering just the nearest BS and the first interferer without shadow fading, (26) in Appendix E shows:

$$\text{Prob}_{\text{Strongest}} \left\{ \frac{C}{I} > y | \epsilon, N \right\} = \frac{N}{N - 1 + y^{2/\epsilon}}. \quad (8)$$

This is an upper bound on performance (it only considers one interferer). Comparing this upper bound for the strongest strategy to the best strategy in (7) we see that performance must be much worse. For instance at the 95th percentile and $\epsilon = 4$, the C/I with $N = 7$ is less than 2.7dB (c.f. Figure 2b). In order to raise this to a 10dB more than 41 CG are required compared to 14 for using the best strategy.

Unlike for the best case, a simple closed form solution that extends to all interferers was not found. Interestingly, the results for the strongest case are independent of shadow fading as shown in Figure 2d.

6.2 Sectoring

So far, we have assumed that the BS use omni-directional antennas. In sectoring, a BS employs multiple narrow-beam antennas each facing a different direction. This reduces the potential interferers and improves the performance of cellular systems [6, 14, 18 p. 57]. In this section, we show that the analysis of sectoring in shotgun systems is particular simple and yields substantial

improvements.

Assume, for simplicity, c ideal sectors each covering $360/c$ degrees of the circle with perfect isolation between signals in each sector and the vertical and horizontal radiation pattern is constant over the arc covered by the sector. Typically $c = 3$. Number the sectors sequentially around the circle, and let ϕ be the angle relative to a reference (e.g. North) of the division between the first and last sector. With independent random orientations, ϕ , and random assignment of the N CG to each BS so that each sector has 1 CG, a BS has a $1/N$ probability of having any given CG facing the MS, i.e. this is identical to the shotgun system without sectoring and so all of the results for the shotgun system apply.

Instead, let the BS agree on the orientation, ϕ , and agree to divide the CG into c sets so that the first set can only appear in sector 1, the second in sector 2, etc., and then BS randomly choose a CG from each set for each sector. The density of BS that are showing a particular sector to the MS and have a given channel assignment for that sector is simply a scaling on the overall BS density. As noted before, such scaling is insignificant in random cellular systems and so coordinating the sectoring has no effect.

Although sectoring does not change the analysis of shotgun systems, every cell now has c CG. In hexagonal systems the CG are grouped and assigned c at a time. In effect, the number of CG for the purpose of channel assignment is $N' = N/c$. In the vernacular of hexagonal cellular systems, c sectors per cell increases the effective number of CG, N , by a factor of c for a given reuse number N' . In hexagonal systems, N' must be determined by simulation for each c . For the shotgun system, c sectors per cell directly increases the effective reuse by a factor of c .

6.3 Channel Assignment:

The shotgun system assigns both CG and BS locations randomly. The same CG can be assigned to nearby adjacent BS resulting in poor C/I in the region between them. While BS locations might be dictated by terrain, political, and economic constraints, in most situations the CG can be assigned better than random. This paper does not intend to give a complete treatment of channel assignment. Many papers exist on the subject of channel assignment and its relationship to graph coloring [1, 9, 15]. The goal is to indicate the potential improvements due to better channel assignments.

Appendix F discusses two channel assignment algorithms. The first is an assignment algorithm based on simulated annealing. The second is a simple algorithm that guarantees that nearest

neighbors are not assigned the same CG. Although simpler it provides half of the performance gains possible compared to the more complex algorithm. Because of the complexity of the simulated annealing based algorithm a method based on the simpler algorithm is used to estimate the complex method's performance and is described in Appendix F. The simpler algorithm has a distributed implementation that makes it suitable for quick or ad hoc deployments. Since it provides half of the potential gains and is easily implemented for any BS geometry, it is recommended for use in its own right.

The gain in shotgun performance with non-random channel assignment is complemented by looking at the loss in hexagonal performance with random channel assignments. This will help disentangle the contribution of BS placement vs. channel assignment.

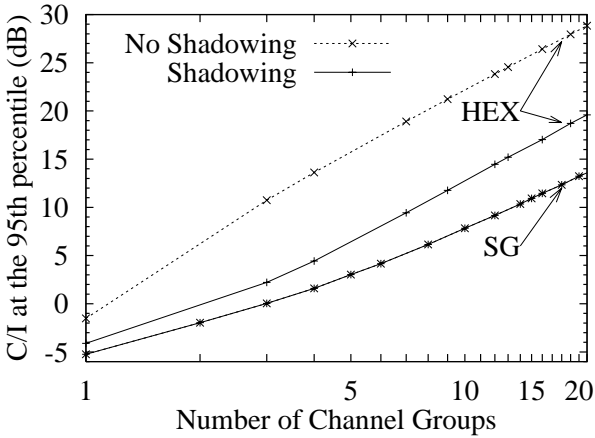
6.4 Hexagonal Layout with Deviations

So far we have assumed that the BS in the hexagonal layout is perfectly aligned with a hexagonal grid. This section looks at designs that might build roughly to a hexagonal grid but place BS within some circle around the true grid point. This circle is sometimes referred to as a *search radius* and we assume that the BS are placed uniformly within this circle. Conceptually, the BS are placed according to an ideal grid and CG are assigned normally. Then, the random deviations are added. Small search circles keep the co-channel interferers well spaced. Large search circles degenerate to the shotgun layout. In this way we can characterize performance as a function of randomness.

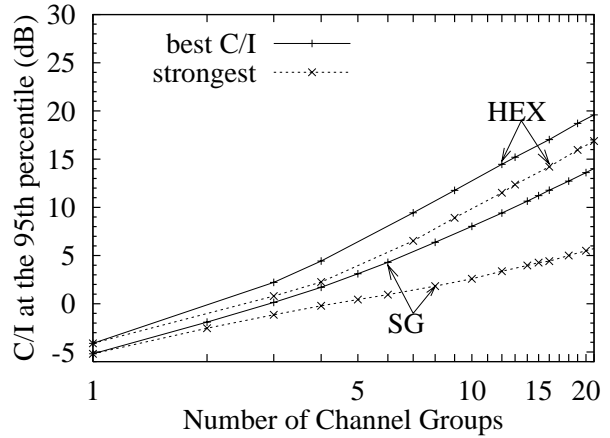
6.5 Performance

This section presents performance results of the shotgun system under several different scenarios. The figures in this section, explicitly show the signal quality (C/I level) versus spectrum efficiency (number of CG) trade-off.

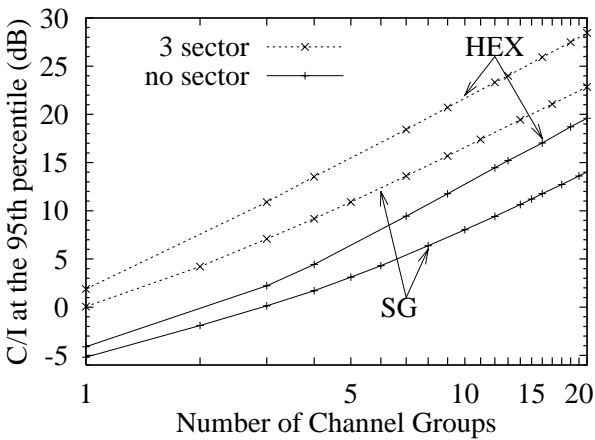
As a baseline case we consider the C/I at the 95th percentile for both the shotgun and hexagonal systems as a function of the number of channel groups. Shadow fading is $\sigma = 10\text{dB}$, the MS uses the Best C/I access strategy, the shotgun uses random CG assignments, and antennas are omnidirectional (no sectoring). Figure 3 shows the baseline case versus five variations: (a) with and without shadow fading; (b) the best vs. the strongest strategy; (c) with and without sectoring into $c = 3$ sectors; (d) with and without channel assignment and (e) increasing deviations from the ideal hexagonal layout.



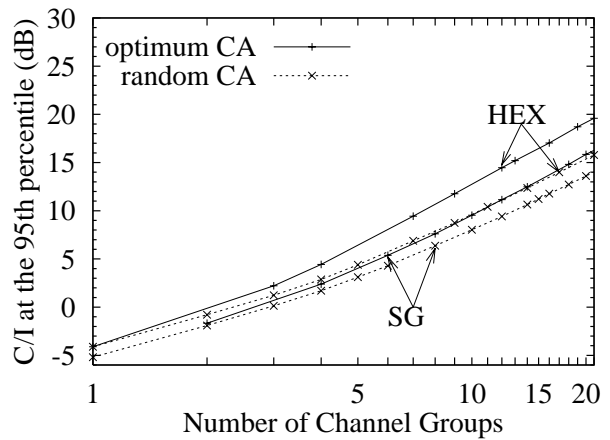
(a) no shadowing vs. $\sigma = 10\text{dB}$ shadowing



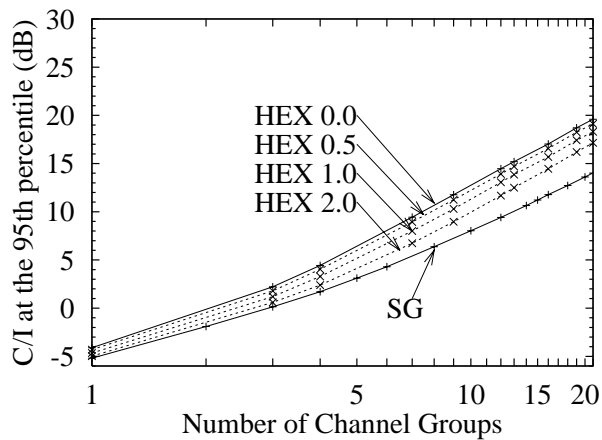
(b) mobile accesses BS with best C/I vs. strongest signal



(c) 1 sector vs. 3 sectors per cell



(d) random vs. optimum channel assignment for the SG system.



(e) HEX with and without placement deviations up to twice the cell radius.

Figure 3: C/I at the 95th percentile for five different design variations with path loss exponent, $\epsilon = 4$.

We first focus on the case of only one CG ($N = 1$). This is important for understanding CDMA cellular systems which reuse every channel in every cell. In the graphs, the upper bound HEX case and the lower bound SG differ by only 1dB. It differs by more in the unrealistic no shadowing case, and in the sectoring case. The sectoring studied in this paper uses different CG in every sector. CDMA systems typically use the same CG in every sector. A proper study of the sectoring effects with one CG in every sector would require a more detailed antenna model. But, we conjecture that the conclusion is the same: With only one CG, all manner of BS layout are about the same under shadow fading.

Now we turn to the $N > 1$ case. Figure 3a emphasizes shadowing's strong detrimental effect on HEX performance. The $\sigma = 10$ dB shadow fading produces an 8-9dB reduction in the HEX C/I. The SG performance is independent of shadowing. In Figure 3b performance degrades for both the HEX and SG when the MS chooses the strongest BS rather than the BS with best C/I. The HEX has 1.5–3dB lower C/I. The SG has 1dB lower C/I for 2 CG, while the gap increases to over 8dB with 21 CG. As noted before, this has a strong detrimental impact on the number of CG needed to reach a given C/I level with 3 times more channels needed to reach a C/I = 10dB at the 95th percentile. Sectoring provides large improvements to both the HEX and SG systems in Figure 3c. The C/I increases by 8-9dB in both cases. The difference between the HEX and SG systems remains unchanged. Figure 3d shows that adding either optimal channel assignment or optimal placement to the SG system increases C/I by 0–2dB. Adding both leads to a total improvement larger than either separately. This indicates that random disturbances to either placement or channel assignment can account for most of the HEX and SG difference.

Figure 3e shows the effect of increasing deviations from ideal on the HEX performance. Deviations up to half the cell radius produce less than 1dB reduction in C/I at the 95th percentile. Deviations up to twice the cell radius produce less than 3dB reduction in C/I. All the reductions fit within the 2–6 dB difference between the HEX and SG performance. For $N \leq 4$ the difference between the HEX and SG systems is effectively eliminated. For larger N , HEX performance clearly exceeds the SG performance. This follows since, for large N , the deviations are small compared to the distance between co-channel BS in the HEX system. The deviations are relative to a uniform hexagonal grid. In practice, cell sizes vary with traffic. These variations effectively create much larger deviations than indicated by the search radius.

The comments so far have focussed on the effects on the C/I at the 95th percentile. Another

important measure is spectrum efficiency—the number of CG to meet a given C/I level. From the graphs the SG system requires approximately 70% more channel to achieve the same C/I level. The SG with the optimal channel assignment requires 40% more.

In summary, the difference between the HEX and SG systems ranges from 6dB when $N = 21$ to less than 3dB when $N = 4$ (typical of newer TDMA digital cellular) and down to 1dB when $N = 1$ (typical of CDMA cellular). Sectoring improves both the HEX and SG systems without changing the difference. The simpler strategy of having MS choose the strongest BS can lead to much worse performance. Non-random channel assignment closes HEX and SG performance gap by 1dB. The gap for smaller N is quickly closed with increasing deviations from the HEX ideal.

7. Discussion

This paper presented a novel look at cellular system design where BS are distributed randomly over the plane, a so called shotgun system. This is argued to be a natural system to analyze as the limit of large perturbations to hexagonal grids or the limit of no-planning in an ad hoc system. As such it provides a lower bound on performance we can expect in practical systems. The shotgun system model is simple enough that it yields a closed form solution for the entire C/I distribution. Further this distribution is shown to have two important properties.

The first is that the distribution is independent of shadow fading. This is shown with empirical evidence and we conjecture that this can be proven analytically. Thus, even when closed form solutions are not available, a simple Monte Carlo analysis with no shadowing is sufficient for any level of shadowing.

The second property is that any system of BS layout and channel assignment reduces to the shotgun system in the limit of large shadow fading standard deviation, σ . Across several scenarios, the difference between the best hexagonal case and the shotgun case is less than 1dB with $\sigma = 18$ dB. Thus in highly variable environments, the random system is nearly as good as the best possible system. Whether this result can be shown analytically is an open question. In a typical environment with $\sigma = 10$ dB, the difference between the hexagonal and shotgun systems ranges from 6dB when $N = 21$ to less than 3dB when $N = 4$ (typical of newer digital TDMA cellular) and down to 1dB when $N = 1$ (typical of CDMA cellular).

The shotgun system is applied to several different scenarios. Sectoring improves both the hexagonal and shotgun systems by 8dB without changing their difference. The simpler strategy of having MS choose the strongest BS can lead to much worse performance. A non-random channel

assignment closes the gap between the hexagonal system and shotgun systems by 1dB.

The shotgun system is most similar to the hexagonal system in the cases of few CG, low required C/I levels, and high signal variability. Cellular technology and applications are all heading in these directions which squeezes the possible performance range of system layouts. In these cases, deviations from the ideal HEX quickly close the performance gap. Given the cost of cell site planning, the possibility of placing sites at the cheapest locations, and the fact that practical system performance is already less than ideal, dispensing with planning may ultimately yield lower system costs.

The analysis in this paper focussed on a relatively simple cellular model. Preliminary analysis shows that the major conclusions in this paper are valid even with more realistic models. Future work will solidify this assertion and consider factors such as the MS to BS path; system dynamics including handoff rates, blocking probabilities, and dynamic channel assignment; realistic antenna patterns; correlated fading models; and transmitter power control. Several empirical results yield simple conclusions. Further work would derive analytic proofs to these results.

APPENDIX A: Properties of Random BS Placement

The shotgun cellular system distributes BS according to a two-dimensional Poisson point process. The average BS density is λ and the probability of a BS in a small area dA is λdA . This appendix develops basic properties of this process.

If K is the random variable for the number of BS in area A :

$$\text{Prob}\{K = k|A\} = \frac{(\lambda A)^k}{k!} e^{-\lambda A}. \quad (9)$$

In particular if A is a circular area of radius r

$$\text{Prob}\{K = k|r\} = \frac{(\lambda \pi r^2)^k}{k!} e^{-\lambda \pi r^2}. \quad (10)$$

From an arbitrary point, the probability of k BS within radius r is given by (10). Let R_k be the distance from an arbitrary point to the k th nearest BS to that point. The probability $R_k = r$ is:

$$p(R_k = r)dr = \text{Prob}\{(K = k - 1|r) \text{ and } (R_k \in [r, r + dr])\} = \frac{(\lambda \pi r^2)^{k-1}}{(k-1)!} e^{-\lambda \pi r^2} \cdot 2\lambda \pi r dr. \quad (11)$$

Taking expectations of (11) with respect to r , the expected distance to the k th nearest BS is:

$$E[R_k] = \frac{\Gamma\left(\frac{1}{2} + k\right)}{(k-1)! \sqrt{\lambda \pi}} = \frac{(2k)!}{2^{2k} k! (k-1)! \sqrt{\lambda \pi}} \approx \sqrt{\frac{k}{\lambda \pi}}. \quad (12)$$

The approximation follows from Stirling's formula. A more general density follows from (11) for M BS. For integers $\{k_1, \dots, k_M\}$ ordered so that $0 < k_i < k_{i+1}$ and using the convention $k_0 = r_0 = 0$:

$$p(R_{k_1} = r_{k_1}, R_{k_2} = r_{k_2}, \dots, R_{k_M} = r_{k_M}) = (\lambda\pi)^{k_M} 2^M e^{-\lambda\pi r_{k_M}^2} \prod_{i=1}^M \frac{(r_{k_i}^2 - r_{k_{i-1}}^2)^{k_i - k_{i-1} - 1}}{(k_i - k_{i-1} - 1)!} r_{k_i}. \quad (13)$$

An important special case is when $M=2$, $k_1=1$, and $k_2=k$. Then

$$p(R_1 = r_1, R_k = r_k) = (\lambda\pi)^k 2^2 e^{-\lambda\pi r_k^2} \frac{(r_k^2 - r_1^2)^{k-2}}{(k-2)!} r_k r_1. \quad (14)$$

Noting that $R_k/R_1 \geq 1$, then for all $y \geq 1$:

$$\text{Prob}\left\{\left(\frac{R_k}{R_1}\right) > y\right\} = \int_{r_1=0}^{\infty} \int_{r_k=r_1 y}^{\infty} (\lambda\pi)^k 2^2 e^{-\lambda\pi r_k^2} \frac{(r_k^2 - r_1^2)^{k-2}}{(k-2)!} r_1 r_k dr_k dr_1 = 1 - \left(1 - \frac{1}{y^2}\right)^{k-1}. \quad (15)$$

This follows by substituting $z_i = \lambda\pi r_i^2$, then substituting $z = z_k - z_1 y^{2/e}$, and then integrating using 3.382.4 followed by 6.451.2 in [12]. These results are used several times through the paper.

APPENDIX B: Computing C/I percentiles via Simulation:

This appendix details this paper's simulation method. The C/I distribution is computed by repeatedly generating cellular layouts, placing a MS, and measuring the C/I of this MS, each repetition representing a trial. Each trial is generated independently of the others and repeats the following steps with options and parameters chosen from Section 2.

- Create a cellular layout with M BS centered on the origin.
- Assign one of N CG to each BS.
- Place the MS.
- Compute the signal strength between the MS and every BS using path loss exponent ϵ , and shadow fading standard deviation, σ .
- Compute the C/I for the MS.

We detail each of these steps in turn. BS are placed either randomly or according to a hex grid. For the random layout, without loss of generality, the MS can be placed at the origin and BS placed in circular coordinates around the origin. Using (13) and Bayes rule, the distances to the nearest M BS are chosen iteratively using the density:

$$p(r_i | r_{i-1}) = \lambda\pi 2 r_i e^{-\lambda\pi(r_i^2 - r_{i-1}^2)} \quad (r_i \geq r_{i-1}), \quad (16)$$

where the first BS is at r_1 and $r_0 = 0$. For each r_i , an angle is chosen uniformly from $[0, 2\pi]$. For

the hexagonal grid, BS are placed in a hexagonal grid with one BS placed at the origin, and the M BS nearest to the origin are retained.

The hexagonal system assigns CG using standard rules [13, 16, 18]. The shotgun system assigns CG either uniform randomly or according to the channel assignment algorithm in Appendix F. The shotgun cellular system places the MS at the origin. The hexagonal system uniformly distributes the MS in the hexagonal cell around the BS at the origin. The remaining elements are computed in a straightforward manner.

The simulations estimate measurement errors as follows. Let the C/I distribution and density be denoted $F(x)$ and $f(x)$. The simulation results are percentiles from the C/I distribution. Given fraction p (e.g. $p = 0.95$ for the 95th percentile) the simulations in this paper estimate $F^{-1}(p)$. Given T trials sorted from x_1 (smallest) to x_T (largest), the estimate is x_n where $n = pT$. As $T \rightarrow \infty$ this statistic is consistent with mean $F^{-1}(p)$, and standard deviation given by [17]:

$$S_F(p, T) = \sqrt{\frac{p(1-p)}{T}} \frac{1}{f(F^{-1}(p))}. \quad (17)$$

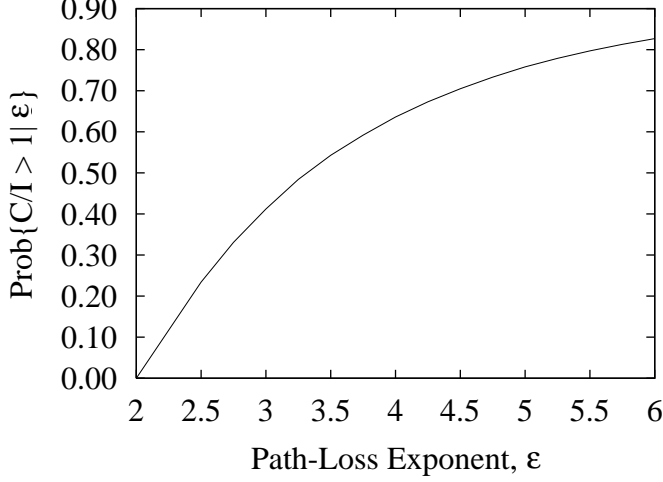
The last factor we estimate using the slope at $F^{-1}(p)$:

$$\hat{f}(F^{-1}(p)) = \frac{n_2 - n_1}{x_{n_2} - x_{n_1}}, \quad (18)$$

where $n - n_1 = n_2 - n = \sqrt{T}$. For instance, when $T = 10,000$ and $p = 0.95$, $n_1 = 9400$ and $n_2 = 9600$. The experiments use $M = 10,000$, and $T = 100,000$. At $T = 100,000$ $\hat{S}_F(p, T) < 0.05\text{dB}$ for all experiments and for clarity error bars are not plotted. Based on Figure 1, and preliminary experiments, $M = 10,000$ has less than 0.1dB difference from larger size systems so that the simulated performance is effectively for cellular systems covering the plane. Appendix F uses $T = 10,000$ in some cases due to computational limits and so the plots there include error bars.

APPENDIX C: Shotgun System C/I Distribution

This appendix derives the C/I distribution for the shotgun cellular system in the limit of infinite number of BS, no shadow fading, and only one CG. Suppose that we want to compute the C/I distribution considering only the k nearest BS and ignoring all other BS denoted $\text{Prob}_k\{C/I > y|\epsilon\}$. This is optimistic with the correct distribution only in the limit of $k \rightarrow \infty$. To get $\text{Prob}_k\{C/I > y|\epsilon\}$ we integrate (13) over the set:



ε	Prob{C/I > 1 ε}
2.0	0.000
2.5	0.250
3.0	0.412
3.5	0.543
4.0	0.636
4.5	0.705
5.0	0.758
5.5	0.797
6.0	0.827

Figure 4: Factor, $K_\varepsilon = \text{Prob}\{C/I > 1 \mid \varepsilon\}$, for computing C/I distribution as a function of ε in (22).

$$S_k(y, \varepsilon) = \left\{ (r_1, r_2, \dots, r_k) \mid \frac{r_1^{-\varepsilon}}{\sum_{i=2}^k r_i^{-\varepsilon}} > y \text{ and } (r_1 \leq r_2 \leq \dots \leq r_k) \right\}, \quad (19)$$

so that

$$\text{Prob}_k \left\{ \frac{C}{I} > y \mid \varepsilon \right\} = \int_{r_1=0}^{\infty} \int_{r_2=\max\{r_1, r_1 y^{1/\varepsilon}\}}^{\infty} \int_{r_3=f_3(r_1 y^{1/\varepsilon}, r_2)}^{\infty} \dots \int_{r_k=f_k(r_1 y^{1/\varepsilon}, r_2, \dots, r_{k-1})}^{\infty} (2\lambda\pi)^k e^{-\lambda\pi r_k^2} \prod_{i=1}^k r_i dr_i, \quad (20)$$

where

$$f_j(x_1, x_2, \dots, x_{j-1}) = \max \left\{ x_{j-1}, \left(x_1^{-\varepsilon} - \sum_{i=2}^{j-1} x_i^{-\varepsilon} \right)^{-1/\varepsilon} \right\}. \quad (21)$$

For $y \geq 1$ (note the limits for r_2), substituting $z_1 = r_1 \sqrt{\lambda\pi} y^{1/\varepsilon}$ and $z_i = r_i \sqrt{\lambda\pi}$ for $i > 1$ into (20) yields two results. The first is that the distribution is independent of λ . This is as expected since ratios of distances do not depend on the distance scale. The second result is that:

$$\text{Prob}_k \{ C/I > y \mid \varepsilon \} = y^{-2/\varepsilon} \text{Prob}_k \{ C/I > 1 \mid \varepsilon \}. \quad (22)$$

This implies that by computing $\lim_{k \rightarrow \infty} \text{Prob}_k \{ C/I > 1 \mid \varepsilon \}$ once, the entire distribution can be computed for a given ε . Numerically integrating (20) for different k and taking limits yields Figure 4 for different ε . As with any cellular system covering the plane, communication is impossible when the path loss exponent is less than or equal to 2. Conversely, C/I only improves with greater attenuation.

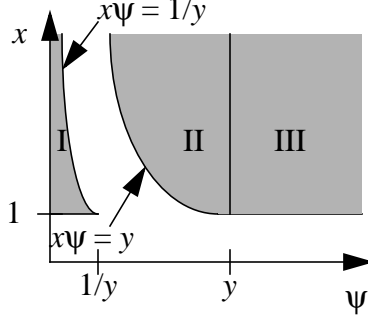


Figure 5: Schematic of the shadowing integral.

APPENDIX D: The Effect of Shadowing:

This appendix derives a closed-form solution to the C/I distribution for the two nearest BS with only one CG. Multiplying or dividing independent log-normal variables produces another log-normal variable in which the means and variances in dB are added. Shadowing multiplies the numerator and denominator of the C/I ratio in (3). With only one interference term in the denominator, the net effect is a single shadowing variable with variance equal to the sum of numerator and denominator shadowing variances. Thus, the net received C/I consists of the product of two random variables, x , the carrier to interference ratio without shadowing, and ψ , the shadowing factor. The density of ψ is given by (1) using a standard deviation of $\sqrt{2}\sigma$, The cumulative distribution for x is given by (4).

It is possible that shadowing makes the further BS stronger than the nearer BS. The effect could be so strong that by choosing the further station, the C/I is high enough for communication. Thus, the set of x and ψ that yield $C/I > y$ are where $x\psi > y$ and $x\psi < 1/y$ subject to the constraint that $x \geq 1$. Pictorially this is shown in Figure 5. Integrating yields:

$$\begin{aligned} \text{Prob}\left\{\frac{C}{I} > y \mid \epsilon, \sigma\right\} &= \left[\int_{\psi=0}^{1/y} \int_{x=1}^{1/(y\psi)} + \int_{\psi=0}^y \int_{x=y/\psi}^{\infty} + \int_{\psi=y}^{\infty} \int_{x=1}^{\infty} \right] p\left(\frac{C}{I} = x\right) p(\psi) dx d\psi \\ &= \text{erfc}\left(\frac{\log y}{2\sigma}\right) + \frac{1}{2} e^{\left(\frac{2\sigma}{\epsilon}\right)^2} \left(\frac{1}{y^{2/\epsilon}} \text{erfc}\left(\frac{2\sigma}{\epsilon} - \frac{\log y}{2\sigma}\right) - y^{2/\epsilon} \text{erfc}\left(\frac{2\sigma}{\epsilon} + \frac{\log y}{2\sigma}\right) \right) \end{aligned} \quad (23)$$

Not a lot of insight can be gathered from staring at this equation other than to note that when $y = 1$ or $\sigma \rightarrow \infty$ it is 1. Requiring $y = 1$ simply means that either the nearest or next nearest is larger than the other. Large σ implies that with high probability ψ lies in regions I, II, or III in Figure 5. As in (4) and (5), this result can be extended to more than one CG.

APPENDIX E: Choosing the Strongest Base Station:

In this appendix, only two BS are modeled and we compute the C/I distribution when the MS chooses the strongest BS. Choosing the strongest BS with no shadowing, means that we take the first BS from any CG, and then choose the next strongest BS from the same CG. Let the CG be assigned randomly to each BS with p_i the probability of assigning CG i to a BS. Let R_{ki} be the distance from an arbitrary point to the k th nearest BS from CG i . Let x_i be the event that the first BS is from CG i and note p_i is the probability of this event. Following equation (10) and (14) from Appendix A and noting that the density of BS from CG i is $p_i\lambda$:

$$\begin{aligned} p(R_{1i} = r_{1i}, R_{ki} = r_{ki}, x_i) &= p(R_{1i} = r_{1i}, R_{ki} = r_{ki}) \prod_{j \neq i} p(R_{1j} > r_{1i}) \\ &= (p_i \lambda \pi)^k 2^2 e^{-p_i \lambda \pi r_{ki}^2} \frac{(r_{ki}^2 - r_{1i}^2)^{k-2}}{(k-2)!} r_{ki} r_{1i} e^{-(1-p_i)\lambda \pi r_{1i}^2} \end{aligned} \quad (24)$$

and

$$\text{Prob}\left\{\left(\frac{R_k}{R_1}\right) > y, x_i\right\} = \int_{r_1=0}^{\infty} \int_{r_k=r_1 y}^{\infty} p(R_1 = r_1, R_k = r_k, x_i) = \left(1 - \left(\frac{y^2 - 1}{1/p_i + y^2 - 1}\right)^{k-1}\right) p_i. \quad (25)$$

Since x_i occurs with probability p_i :

$$\text{Prob}\left\{\left(\frac{R_k}{R_1}\right) > y\right\} = \sum_{i=1}^N \text{Prob}\left\{\left(\frac{R_k}{R_1}\right) > y, x_i\right\} = \sum_{i=1}^N \left(1 - \left(\frac{y^2 - 1}{1/p_i + y^2 - 1}\right)^{k-1}\right) p_i. \quad (26)$$

For $k = 2$, (26) can be shown to be maximized when for all i , $p_i = 1/N$. Maximizing this for $k > 2$ is still open.

APPENDIX F: Two Channel Assignment Algorithms

This appendix presents two algorithms for assigning one of N CG to each BS. The first algorithm is computationally expensive and indicates performance with an optimization algorithm. A second, simpler algorithm is presented that we use to estimate performance with the more complex algorithm. This latter algorithm has merit in its own right since a distributed implementation is possible. In principle the algorithms could be applied to the hexagonal system. Since simple optimal assignments exist, these algorithms are only used in the shotgun case.

Channel Assignment Based on Optimization:

The first algorithm is a stochastic optimization algorithm related to simulated annealing and genetic algorithms based on the population-based incremental learning (PBIL) algorithm [1]. This is just one of a number of possible simulated annealing type algorithms and the details are

included here simply for completeness. The algorithm starts with a uniform distribution of channels for each BS. A population of random channel assignments is chosen from the distribution. Each assignment is evaluated with an objective function. The channel distribution for each BS is biased towards the assignments in the best member of the population. A new population is chosen and the process repeated. Some care must be taken so that the distribution does not converge too quickly. A lower probability limit is set so that every channel has at least this probability of being chosen. This limit is initially set high and slowly reduced.

The objective function used for this problem is based on the interference between nearest neighbors defined as follows. Given M BS, a function $K(i, j)$ which indexes the i th BS's k th nearest neighbor, $D(i, j)$ the Euclidean distance between the i th and j th BS, an integer $B \leq M$, and a set of channel assignments to the BS, $C = (c_1, c_2, \dots, c_M)$, the objective function is:

$$J(C) = \sum_{i=1}^M \sum_{k=1}^B \delta(c_i, c_{K(i,k)})(D(i, K(i,k)))^{-\epsilon}, \quad (27)$$

where $\delta(\cdot, \cdot) = 1$ if the arguments are equal and zero otherwise. This objective has a minimum of zero if the B closest neighbors to every BS have a different channel assignment. Violations to this are weighted in (27) so that the penalty for co-channel assignments are proportional to their BS-BS co-channel interference.

Using this objective function, pseudocode for the algorithm is listed in Figure 6. The optimization parameters used throughout the paper are chosen by a grid search over possible values and are also given in Figure 6. The number of nearest neighbors, B , is also a parameter. Experimentally, if $B < N$, a non-interfering channel assignment could be found quickly with probability greater than 99.5%. A non-interfering channel assignment is never found for $B > N$, although performance improved. $B = 2N$ is used in the experiments since larger B produced only minimal performance gains while incurring computational penalties.

Given the parameter choices, the complexity of the algorithm is $O(NM^3)$. For 200 BS, 8 colors, and 10,000 trials, this algorithm required several days on a 300MHz Sun workstation. Scaling to the 10,000 BS used in the experiments would have involved 10's of weeks. This led to using the simple coloring algorithm in the next section.

A Channel Assignment Algorithm Based on Nearest Neighbors:

A simple assignment algorithm that works well with this problem is presented. For two CG we

Figure 6: Pseudocode for the stochastic search coloring algorithm.

ASSIGN_CHANNEL(int M , int N)

```

 $J(C)$  Parameters: int  $M$ , int  $B$ , real matrix  $D$ , int matrix  $K$ , real  $\epsilon$ .

Optimization Parameters: population_size =  $M/2.5$ , num_generations =  $4M$ ,
start_limit =  $0.5/N$ , anneal_rate =  $0.178^{1/M}$ , change_rate = 0.80.

Initialize:  $p(i, n) = 1/N$  for  $1 \leq i \leq M$ ,  $1 \leq n \leq N$ , and prob_limit = start_limit.

for num_generations iterations repeat {
    Choose population_size sample colorings,  $\{C^m\}$ , where  $\text{Prob}(c_i^m = n) = p(i, n)$ .

    Choose  $C^m$  that minimizes  $J(C^m)$ 

    for each  $i \in \{1, \dots, M\}$  {
        sum = 0.
        for each  $n \in \{1, \dots, N\}$  if ( $n \neq c_i^m$ ) {
             $p(i, n) = \text{MAX}\{\text{change\_rate} \cdot p(i, n), \text{prob\_limit}\}$ .
            sum = sum +  $p(i, n)$ .
        }
         $p(i, c_i^m) = 1 - \text{sum}$ ;
    }
    prob_limit = prob_limit * anneal_rate
}
Return  $C$  that had lowest  $J(C)$ .

```

use the following theorem.

Theorem: Two colors can always color any set of points so that a point and its nearest neighbor always have different colors. No particular metric is assumed here as long as the nearest neighbor is unique.

Proof: The nearest neighbors induce a directed (not necessarily connected) graph with nodes corresponding to the points and edges connecting from a node to its nearest neighbor. Thus all nodes have out-degree 1. Nodes are colored as follows. Choose the two nearest points in the graph. They must be connected to each other. Choose one as a root. A tree is grown as follows. By construction, connections from nodes already in the tree connect to other nodes in the tree. Thus any node adjacent to the tree must be directed toward the tree. Adding adjacent nodes one by one by induction forms a tree with all nodes having a unique directed path toward the root. When no more nodes are adjacent, the tree can be colored with two colors starting at the root and colors alternating with levels. Remove the tree's nodes from consideration and a new tree can be grown with the remaining nodes. Q.E.D.

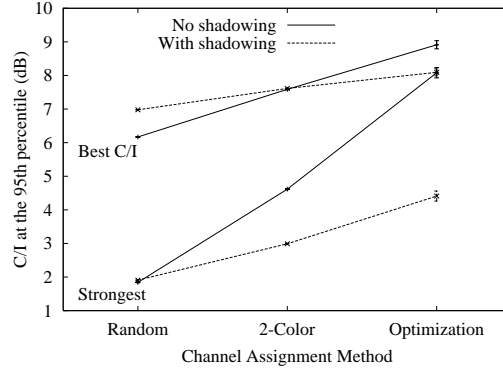


Figure 7: Performance of random cellular layout with 200 BS and 8 CG for three different channel assignment algorithms. The lines are added to aid comparisons.

The method can be extended to more than two CG. Let the number of CG, N , be even. Randomly assign the N CG to the BS. Partition the CG into $N/2$ pairs. For each pair, treat the subset of nodes with this pair's CG independent from the other nodes and reassign the CG pair according to the theorem.

While the channel assignment complexity is linear in M , the number of BS, the overall complexity is dominated by the $O((M/N)^2)$ complexity of finding the nearest neighbors within each color pair. We describe a simple distributed implementation. Every BS determines its nearest neighbor based on signal strength. Two BS know they are at the root of the induced tree if they are nearest neighbors to each other. The two CG are assigned to these BS. After this initial stage the assignment proceeds in rounds. In each round, the unassigned BS probe their neighbor. If the neighbor has a channel assignment, the BS assigns itself the other CG. Otherwise, the BS waits. These rounds continue until all BS have a CG. Since at least one BS is colored in each round, no more than M rounds are needed. In practice the process completes in half a dozen rounds.

Estimating performance of an optimal coloring:

Figure 7 shows the performance of the Random, Two-Color, and Optimization based channel assignment for 200 BS and 8 CG. We note three observations. Channel assignment yields larger improvements without shadowing than with shadowing (3 times more). Channel assignment yields larger improvements when the MS chooses the strongest CG then when it chooses the CG with the best C/I (2 times more). Finally, the improvement with the optimization is always at least twice as much as the improvement with the Two-Color method. These observations are typical of several experiments with different numbers of BS and colors. The latter observation we use for an important simplification in our experiments. Let x_R , x_2 , and x_O be the performance in decibels

with Random, Two-Color, and Optimization channel assignment for a given experiment. Since x_O is computationally limited, we estimate

$$\hat{x}_O = x_R + 2(x_2 - x_R) = 2x_2 - x_R \quad (28)$$

Given the above observation, this estimates performance with an optimal channel assignment.

Acknowledgment:

This paper began with discussions and experiments with Phillip T. Porter. Harold N. Gabow provided insights into the coloring algorithms. An earlier version of this paper appears in [3].

References:

- [1] Baluja, S., "Genetic algorithms and explicit search statistics," in *Advances in Neural Information Processing Systems*, 9, Mozer, M.C, et al. ed. MIT Press, 1997. pp. 319–325.
- [2] Bernhardt, R.C., "Performance aspects of two-way transmission in portable radio systems," *Proc. IEEE VTC'89*, San Francisco, CA, May 1–3, 1989, pp. 279–284.
- [3] Brown, T.X., "Analysis and Coloring of a Shotgun Cellular System," in *Proceedings of the IEEE Radio and Wireless Conference (RAWCON) 98*, IEEE pub, 1998, pp. 51–54.
- [4] Brown, T.X., "Dynamic Channel Assignment in Shotgun Cellular Systems," in *Proceedings of the IEEE Radio and Wireless Conference (RAWCON) 99*, IEEE pub, 1999, pp. 147–150.
- [5] Chamaret, B., et al., "A randomized algorithm for graph coloring applied to channel allocation in mobile telephone networks," *Proc. of the 6th Annual Conf. on Operational Research*, pp. 25–30, Oct. 1996.
- [6] Chan, G.K., "Effects of sectorization on the spectrum efficiency of cellular radio systems," *IEEE T. on Vehicular Technology*, v. 41, n.3, pp. 217–25, Aug. 1992
- [7] Cox, D.C., "Universal Digital Portable Radio Communications," *Proc. of the IEEE*, v. 75, n. 4, pp. 436–477, Apr. 1987.
- [8] Cox, D.C., "A radio system proposal for widespread low-power tetherless communications," *IEEE T. on Comm.* v. 39, n. 2, pp. 324–335, Feb. 1991.
- [9] Duque-Anton, M., et al., "Channel assignment for cellular radio using simulated annealing," *IEEE. T. on Vehicular Technology*, v. 42, n. 1, p. 14–21, 1993.
- [10] Freeman, R.L., *Radio System Design for Telecommunications, 2nd Ed.*, John Wiley & Sons, 1997.
- [11] French, R.C., "The effects of fading and shadowing on channel reuse in mobile radio," *IEEE. T. on Vehicular Technology*, v. 28, n. 3, pp. 171–81, Aug. 1979.
- [12] Gradshteyn, I.S., Ryzhik, I.M., *Tables of Integrals, Series, and Products, Fifth ed.* Academic Press, 1994.
- [13] Lee, W.C.Y., *Mobile Communications Design Fundamentals, 2nd Ed.*, John Wiley & Sons, 1993. p. 210.
- [14] Macdonald, V.H. "The Cellular Concept," *The Bell System Technical Journal*, v. 58, n. 1, Jan 1979, pp. 15–41.
- [15] McEliece, R.J., Sivarajan, K.N., "Performance limits for channelized cellular telephone systems," *IEEE T. on Information Theory*, v. 40, n. 1, p. 21–34.
- [16] Mehrotra, A., *Cellular Radio: Analog and Digital Systems*, Artech House Pub., 1994. p. 34.
- [17] Mood, A.M., Graybill, F.A., Boes, D.C., *Introduction to the Theory of Statistics 3rd Ed.* McGraw Hill, 1974. p. 257,
- [18] Rappaport, T.S., *Wireless Communications: Principles and Practice*, Prentice Hall, 1996. p. 38.
- [19] Seidel, S.Y., et al., "Path loss, scattering, and multipath delay statistics in four European cities for digital cellular and microcellular radio telephone," *IEEE T. on Vehicular Technology*, v. 40, n. 4, pp. 721–730, Nov. 1991.
- [20] Seidel, S.Y., et al., "914 MHz path loss prediction models for indoor wireless communications in multifloored buildings," *IEEE T. on Antennas & Propagation*, v. 40, n. 2, pp. 207–217, Feb. 1992.
- [21] Sklar, B. "Rayleigh fading channels in mobile digital communication systems Part I: Characterization" *IEEE Comm Mag.*, pp. 90–109, Jul. 1997